Assessment of Madymo Active Human Body Model Kinematics and Dynamics by means of Human Volunteer Response at Low-Speed Frontal Impacts

Manuel Valdano, Jesús R. Jiménez-Octavio, Carmen M. Vives-Torres, Francisco J. López-Valdés, Bengt Pipkorn

Abstract   The aim of this study was to evaluate the capability of the Madymo active HBM to predict the human response by comparing the predictions from the model with the response from human volunteers in frontal-impact tests at 9km/h. The Madymo active HBM correspond to a 50th percentile male model population (standing height=176cm; weight=75.3kg) and the 13 volunteers were selected to have a similar anthropometry (standing height=173.0±4.3cm; weight=79.1±9.5kg). The influence of a number of important parameters on the Madymo active HBM predictions was evaluated. Those parameters were friction between model and seat pan, reaction time delay and level of co-contraction of neck muscles. The friction was varied between 0.15 and 0.5; the reaction time delay from 0ms to 100ms and the level of co-contraction of neck muscles between a null and full activation. The benchmark considered the displacements of the head, vertebra (C4, T1, T4, T8, T12) and hip, the belt loads, and the estimated upper neck loads in the sagittal plane. It was found that while variations in the RT and CCR levels could cause similar forward excursions, this could also result in an overprediction of the downward excursions; and therefore, the neck muscle controller optimization should always consider both. Two configurations could be implemented in the model to represent the large variation between the volunteers' downward excursion, the first with the closest behaviour to the volunteers' mean and the second closer to the volunteers which showed larger head excursion.

Keywords   frontal impact, active human body model, multibody, muscle activation.

I.   INTRODUCTION

The use of Human Body Models (HBM) enables an understanding of injury mechanisms and of how modifications of restraints and vehicles influence injury risk in different crash scenarios. They can be considered a more advance tool to mimic the human response in a crash compared to anthropomorphic test devices (ATD, or crash test dummies). Furthermore, the use of HBM allows to run large parametric studies that consider the variability of crash parameters and occupants' characteristics existing in the real world [1–5]. Another advantage of HBM is the possibility of including muscle activation in their response, which enables to study the effects of breaking or avoidance manoeuvres on the occupant posture and the change in injury risk in a potential subsequent crash [6,7]. Therefore, it is important to benchmark active HBMs against experiments performed with human volunteers, in which muscle controller parameters can be tuned so that the HBM response matches the volunteers' response. To this end, frontal sled acceleration tests with a passenger [8–10] and a driver configuration [11], and sled rear-end acceleration tests [12] have been used to improve the biofidelity of HBM.

Several commercially available HBMs have been used to predict the active human mechanical response, such as : the multibody Madymo active HBM [13], and finite element models as the THUMS v5 [14] and v6 [15], the VIVA model [16], and the GHBMC model [17]. Previous studies with volunteers exposed to frontal deceleration pulses peaking between 0.8-15g have been used to validate HBMs in both relaxed and braced conditions [13–15,17,18]. In these benchmarks between the experiments and the HBM simulations, the surrogate validation usually relies on the head, neck, and torso excursion, head rotation and forces such as contact forces, steering wheel force, and belt forces. However, not all of them provide a comparison of the vertical head displacement

or, if they do, the HBM predictions show a lower correlation with the experimental observations than the one obtained for the longitudinal direction [6,16]. This could lead to a different occupant posture after a breaking event, and therefore to a wrong optimization of the coupling between active and passive safety devices.

The Madymo active HBM is a whole-body multibody (MB) model and has been validated to predict the human behaviour in relaxed and braced conditions [13,19–21]. The validation process was carried out with peak accelerations of 1g for car braking events and 3.8g and 15g for frontal impacts, in a relaxed condition. The 3.8g frontal impact validation showed that the peak volunteer forward excursion of the head top, T1 vertebra, and iliac crest, exhibited less than 20% deviation from the corresponding volunteers' corridors. For this validation data set, the best fit of the volunteers' response was obtained with a 25ms reaction time delay and a half level of co-contraction of the neck muscles, where the first parameter contemplates the time required by the volunteer to notice a change in the posture and the latter considers the activation of flexor and extensor neck muscles at the same time producing a null neck moment. However, these validations were only performed for the forward excursions.

The aim of this study was to assess the kinematic and dynamic response of the Madymo active HBM with a new set of kinematic data corresponding to frontal deceleration tests at 9km/h (3.8g peak acceleration) of 13 male adult human volunteers with a wide age range (18-82 years old).

II. METHODS

Experimental Test Setup and Crash Pulse

The published volunteer data in low-speed frontal impacts from Vives-Torres et al. [22] were used as reference data. This experiment used a similar setup and acceleration pulse than the used in previous validation [8], but the former has more data available to benchmark the model. It was used a test fixture for the experiment with volunteers which was designed to represent the seating posture of a passenger car occupant in a simplified manner. It consisted of a rigid seat, a rigid footrest, a flexible back rest made of three segments of metal wire, and two rigid low backrest supports. This test fixture had been already used with other surrogates in addition to human volunteers (the THOR dummy, PMHS tests) [22–24]. The fixture was designed to facilitate modelling the tests, consisting of rigid parts (seat, footrest) and a non-retractor three-point seat belt. The position of the footrest and of the seat belt D-ring were adjusted depending on each volunteer's anthropometry to ensure that the loading scenarios were dynamically similar [25]. The magnitude and the time history of the sled deceleration were chosen based on previous studies to ensure a safe experimental environment for the volunteers [8,26]. The volunteer study was reviewed and approved by CEICA, the regional government institution that regulates and assess the Ethics of clinical studies with human subjects in the region of Aragon (Spain). The test pulse is shown in Figure 1.
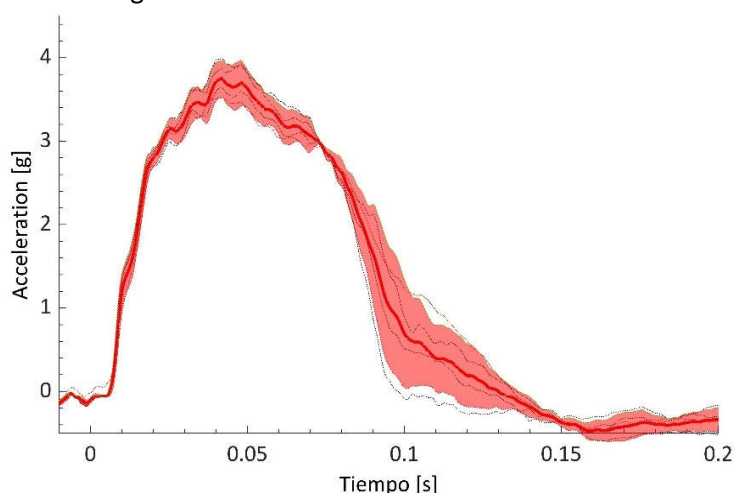

Figure 1. Sled acceleration pulse used to carry out the experiment. The solid line is the average sled deceleration while the shaded area corresponds to the corridor that includes ±1 standard deviation of the measured sled deceleration of each volunteer test.

The volunteers were instrumented with reflective markers, which were attached to selected anatomical landmarks. The 3D displacement of these markers was collected at 1,000Hz using an optoelectric

stereophotogrammetric system consisting of 10 cameras (Vicon, TS series, Oxford, UK). In addition, a head mount that included a triaxial accelerometer cube (Endevco 7264C, Meggitt, Irvine, 81 US) and a triaxial angular rate sensor (ARS PRO-18K, DTS, Seal Beach, US) was attached to an adjustable headband. Three load cells were mounted in the fixture: one under the seat plate and one under each footrest.

The anthropometric measurements as well as additional information of the volunteers that participated in the experiments are included in [22]. The main average volunteers' anthropometric characteristics were: standing height=173.0±4.3cm; weight=79.1±9.5kg; head mass=4.20±0.13kg; and head moment of inertia=0.0251±0.0028kgm2.

Definition of coordinate systems

Five coordinate systems were used in agreement with [22], as it is shown in Figure 2. The position of the reflective markers was measured with respect to a fixed global coordinate system (GCS) in the experiments, which was fixed to the laboratory. The position of these markers was calculated with respect to the local coordinate system (LCS), which was fixed to the sled, to calculate their displacement in this reference. The third reference frame, the neck coordinate system (NCS), was place at the occipital-condyle junction to describe the neck response of the volunteers and the HBM. The orientation of the NCS was determined so that it would meet the criteria stablished in the SAE J211 standard [27]. In addition, the last two reference frames were positioned at the load cells of the seat (SCS) and the footrest (FCS).
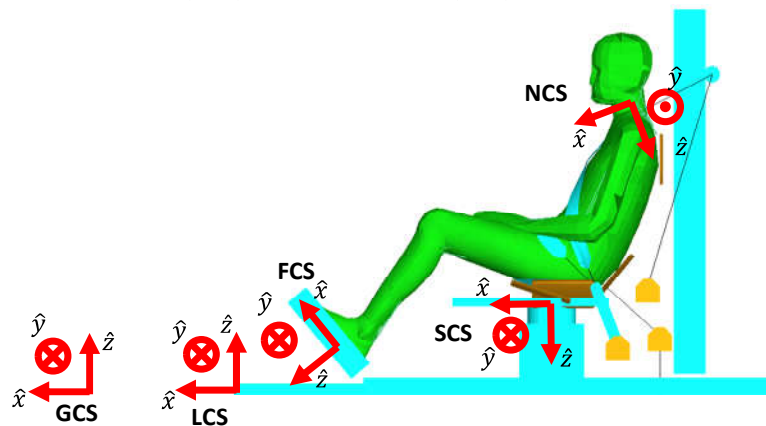

Figure 2. Position and orientation of the coordinate systems used in the study. GCS: global coordinate system (attached to the laboratory); LCS: local coordinate system (attached to the sled); FCS: footrest coordinate system (attached to the footrest load cells); SCS: seat coordinated system (attached to the seat load cell); NCS: neck coordinate system (attached to the occipital-condyle).

Model setup

The computer model used to carry out the study consisted of two systems: the test fixture system and the active HBM. The first one represents the test fixture used in the project SENIORS [22–24] and it was adapted from the model developed by Sebastian Büchner [28] in Virtual Performance Solution (ESI Group, Paris, France) to be used in Simcenter Madymo[TM] (Helmond, The Netherlands). The sled model is composed by rigid shell elements and the wire backrest used at the experimental setup was modelled with a hyper-ellipsoid and its position was determined so that the model would reach the same initial posture as the volunteers in the tests. In addition, three hyper-ellipsoids were placed parallel to the test rig surface, to stablish the contact between the seat and the HBM, and another one parallel to the low back of the HBM, to represent the low backrest supports. The seat belt webbing was modelled as a 50mm wide and 20kN of tension at 10% elongation.

The second system of the model was the Madymo active HBM v3.2 [13], which represents 50th percentile male model population, developed by Siemens Madymo. This HBM has the following anthropometric measurements: standing height=176cm; weight=75.3kg; head mass=4.69kg; and head moment of inertia=0.0236kgm^2. Muscles are modelled with Hill-type elements and are commanded by a PID controller with two-time delays. The first one is before the PID controller, which is the reaction time delay (RT), which models the awareness of the model, and it can be modified by the user. The second one is after the PID controller, which is the neural delay. In addition, Siemens Madymo enables the active HBM to include the co-contraction (CCR) of the neck muscles, which is the contraction of extensor and flexor neck muscles without giving any

resultant moment.

The initial posture of the HBM was set up to match the average initial posture measured in the volunteer tests and the following reflective markers were considered: the ankles, knees, pelvis, shoulder, head, elbow, and C4, T1, T4, T8, and T12 vertebra. The initial orientation of the pelvis was determined through the angle measured between the line connecting the hip joint and the ASIS and the horizontal XY plane of the sled. The initial orientation of the thigh and lower leg were determined to match the 15° and 60° angles defined between the horizontal plane and the upper-thigh and the frontal-lower leg surface, respectively. A pre-simulation was performed under the action of the gravity until the model reached a stable initial position. An initial pretension of 50N was applied to the seat belt similarly to what had been done in the volunteer tests. The friction coefficients used in the model were shoes-footrest equal to 0.6 and seatbelt-HBM equal to 0.2 and 0.5 in the seatbelt longitudinal and transversal direction, respectively. Figure 2 shows the final position of the HBM on the test fixture.
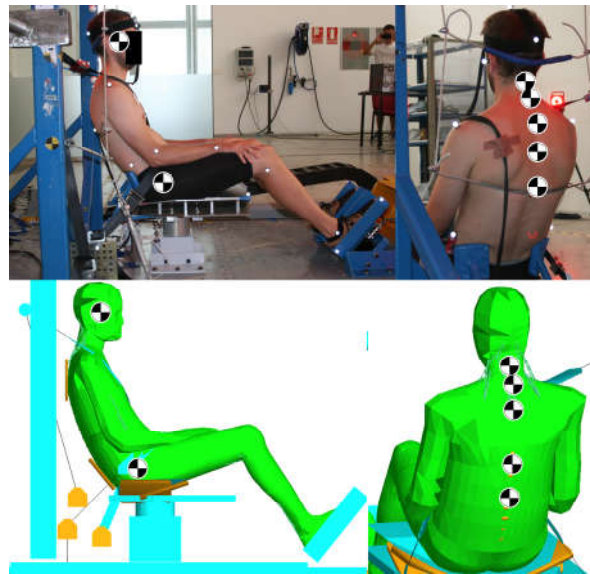

Figure 3. Head, hip, and C4, T1, T4, T8, and T12 vertebra markers in a volunteer and the HBM.

Quantitative Assessment of the Kinematics and Neck Response

The quantitative assessment of the performance of the HBM was carried out using several kinematic and dynamic quantities either measured or calculated from the volunteer experiments: forces measured at the seatbelt, the seat and the footrest; displacements captured from the reflective markers for selected anatomical locations; head rotational acceleration and the evaluation of the neck forces and moment in the sagittal plane [22]. Displacements perpendicular to the sagittal plane were dismissed, and therefore the assessment of the displacements of the markers were performed in the X-Z plane of the LCS. Furthermore, the neck response was computed as the axial force, the shearing force (in the sagittal plane), and the bending moment (perpendicular to the sagittal plane) measured at the occipital-condyle junction.

Peak values and their corresponding timing were used to benchmark the external forces acting on the occupant and the excursions of selected body landmarks. The forces were measured in the seatbelt, at the shoulder belt (upper and lower sensor) and lap belt (inner and outer sensor), and the seat and footrest contact forces were recorded in the X axis of the SCS and the Z axis of the FCS, respectively. Furthermore, corridors were obtained for the belt forces and contact forces using the CORA method [29,30], using +/-0.5 and +/-1 standard deviation (SD) to determinate the inner corridors and the outer corridors, respectively. This process was also applied to the rest of signals and their results can be found in Table IV in the appendix. The assessment of the excursions was carried out for the head, hip, and C4, T1, T4, T8, and T12 vertebrae markers, which are shown in Figure 3. The vertebrae marker positions were measured with points in the HBM skin. For this process, the node selected was the one in the back or neck skin, which was at the same height as the vertebrae. As with the seatbelt and contact forces, the CORA method was applied to obtain the corridors for the neck forces (Fx and Fz) and moment (My) and the angular head acceleration. The following filters were applied to the output signals: displacements-180 CFC; seatbelt forces-60 CFC; contact forces-60 CFC; neck forces-1000 CFC; neck moment-600 CFC; head angular acceleration-60 CFC.

Boundary Conditions and HBM muscle control parameters

The simulations were carried out in three groups to study the effect of variations in the muscle action configuration and boundary conditions on the HBM's response. In the first stage three frictions coefficients were tested (μ=[0.15, 0.3, 0.5]) with no CCR of the neck muscles and RT=0ms to measure the effect of this parameter on the HBM kinematic and exterior loads. The rest of simulations included variations in the RT and CCR of the neck muscles to assess their predictions against the volunteers' response. Firstly, four RT configurations were tested (RT=[0, 25, 50, 100]ms) with no CCR of the neck muscles. Lastly, different combinations of RT and CCR of the neck muscles were tested. Furthermore, the combinations tested were four simulations with a full co-contraction and the same time of responses evaluated in the second group and a single simulation with half level of co-contraction and a time of response equal to 25ms, which had obtained the best fitting in a previous study [13]. Pre-simulation times were selected from preliminary tests of the models to determine the time required to reach a stable posture. The combination of pre-simulation time, boundary conditions and HBM configuration are shown in the table below.

TABLE I
BOUNDARY CONDITIONS AND HBM CONFIGURATION USED TO CARRY OUT THE SIMULATIONS

Simulation	Pre-simulation time (s)	Friction coefficient	RT (ms)	CCR
01	0.2	0.3	0	No
02	0.2	0.15	0	No
03	0.2	0.5	0	No
04	0.2	0.3	25	No
05	0.3	0.3	50	No
06	0.5	0.3	100	No
07	0.2	0.3	0	Full
08	0.2	0.3	25	Full
09	0.2	0.3	50	Full
10	0.2	0.3	100	Full
11	0.2	0.3	25	Half

III. RESULTS

Eleven simulations were carried out varying the friction coefficient, the time of response, and level of co-contraction of the neck muscles of the Madymo active HBM. Several physical quantities were used to benchmark the outcome of the model with the results obtained from experiments performed with thirteen adult volunteers in a 3.8g peak acceleration frontal impact.

Figure 4 shows the sagittal position of the reflective markers of the volunteers and the position of equivalent points of the HBM for the eleven simulations at t=0ms. The mean and a standard deviation of the initial positions of these markers were also included through black-line squares. The marker positions were measured in the LCS of the sled and the volunteers' markers showed in the figure are: the midpoint between the markers located at either side of the head; the markers of the C4, T1, T4, T8, and T12 vertebra; and the midpoint between the markers located at either side of the hip joints. In the case of the HBM were measured: the position of the head centre of gravity (COG); the position of the HBM facet nodes next to the C4, T1, T4, T8, and T12 vertebra; and the position of the hip joint. On average, hip and head reached similar positions, but there was larger dispersion with the vertebrae markers.

Evaluation of the influence friction coefficient

Three friction coefficients were evaluated (μ=[0.15, 0.3, 0.5]). Table II shows the peak forces for the shoulder belt (ShB) and lap belt (LapB) and peak excursions for the head, C4 and T12 vertebrae, and hip joint obtained for each friction coefficient. The variation of the friction coefficient did not show a noticeable influence (>5%) in the head and neck kinematics. However, variations observed in the lap belt forces and hip joint excursion were around ±20% and were around ±10% for the shoulder belt. Although the mean volunteers' peak lap belt force was overpredicted by 50% for the lower friction coefficient, it was slightly higher than the volunteers' corridor. In the case of a high friction coefficient, the hip joint mean excursion was underpredicted by 13mm and peak lap belt force had a difference lower than 5%. The difference in timing of the peaks (Tpeak) were under 10ms

with respect to the volunteers, except for the X-hip joint and Z-head displacements, which were from 15ms to 28ms.
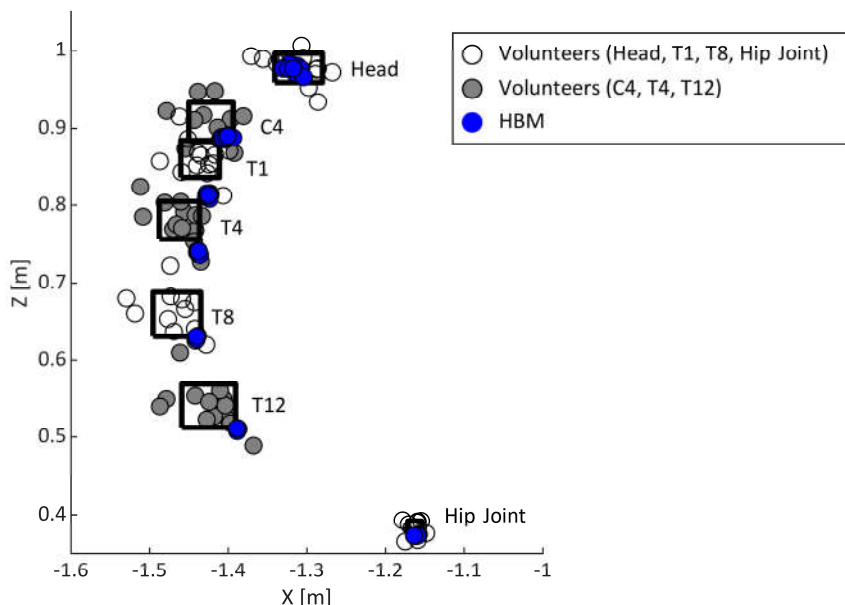

Figure 4. Initial position of reflective markers for the volunteers (white and grey dots) and for the eleven simulations with the active HBM (blue dots). The black-line squares represent the mean initial position of the volunteers' markers plus a standard deviation in the vertical and horizontal direction.

TABLE II
PEAK BELT LOADS AND EXCURSIONS OF SIMULATIONS WITH DIFFERENT FRICTION COEFFICIENTS AND VOLUNTEERS' MEAN

Friction coefficient		Volunteers' mean	μ=0.15	μ=0.3	μ=0.5
Upper ShB	Peak [N]	1263±197	1213	1163	1056
	Tpeak [ms]	95±9	87	86	85
Lower ShB	Peak [N]	1200±159	965	920	820
	Tpeak [ms]	93±9	88	85	85
Inner LapB	Peak [N]	710±117	994	791	631
	Tpeak [ms]	92±10	90	88	82
Outer LapB	Peak [N]	680±140	909	741	627
	Tpeak [ms]	89±9	92	85	85
Head X	Peak [mm]	134±14	120	122	125
	Tpeak [ms]	156±21	153	153	152
Head Z	Peak [mm]	-47±17	-54	-55	-56
	Tpeak [ms]	184±37	194	203	212
C4 X	Peak [mm]	103±13	87	89	92
	Tpeak [ms]	152±16	147	147	147
T12 X	Peak [mm]	53±13	30	27	25
	Tpeak [ms]	101±12	96	93	95
Hip X	Peak [mm]	36±12	33	28	22
	Tpeak [ms]	110±11	95	92	95

Figure 5 shows the shoulder belt and lap belt forces (upper shoulder belt and outer lap belt) and the seat and footrest contact forces (seat contact force: X direction of SCS; footrest contact force; Z direction of FCS). As shown in Figure 5, the upper shoulder belt prediction correctly fitted the volunteers' corridor and for the outer lap belt only the lower friction coefficient produced a slightly higher force than the one measured in the volunteers. A similar behaviour was obtained for the contact forces at the seat and footrest, where the predictions correctly matched volunteers' corridors. However, the seat contact force had a shorter duration than the volunteers' ones.

Evaluation of HBM time of response

The simulations performed to test the different HBM RT were carried out with a friction coefficient equal to 0.3, null CCR, and four reaction time delays (RT = [0, 25, 50, 100]ms). As shown in Figure 6, an increment in this parameter produced an increment of the head excursion in both axes. The null RT showed the best correlation with the volunteers' excursion (X=[134±14mm at t=156±21ms]; Z=[-47±17mm at t=184±37ms]) with a forward excursion of 122mm (t=153ms) and a downward excursion of 55mm (t=203ms). In the cases with higher RT, the head excursion was overpredicted with the larger difference occurring in the downward excursion. The peak forward excursion obtained with higher RT incremented from 28 to 45% (34-56mm) with respect of the RT=0ms. Moreover, the configuration with RT=100ms, which showed the larger forward excursion, overpredicted the larger volunteers' forward excursion (159mm) by 12%. However, the simulations with RT=[25, 50, 100]ms overpredicted the mean volunteers' downward excursion from 123 to 148% with [102; 121; 113]mm, respectively.
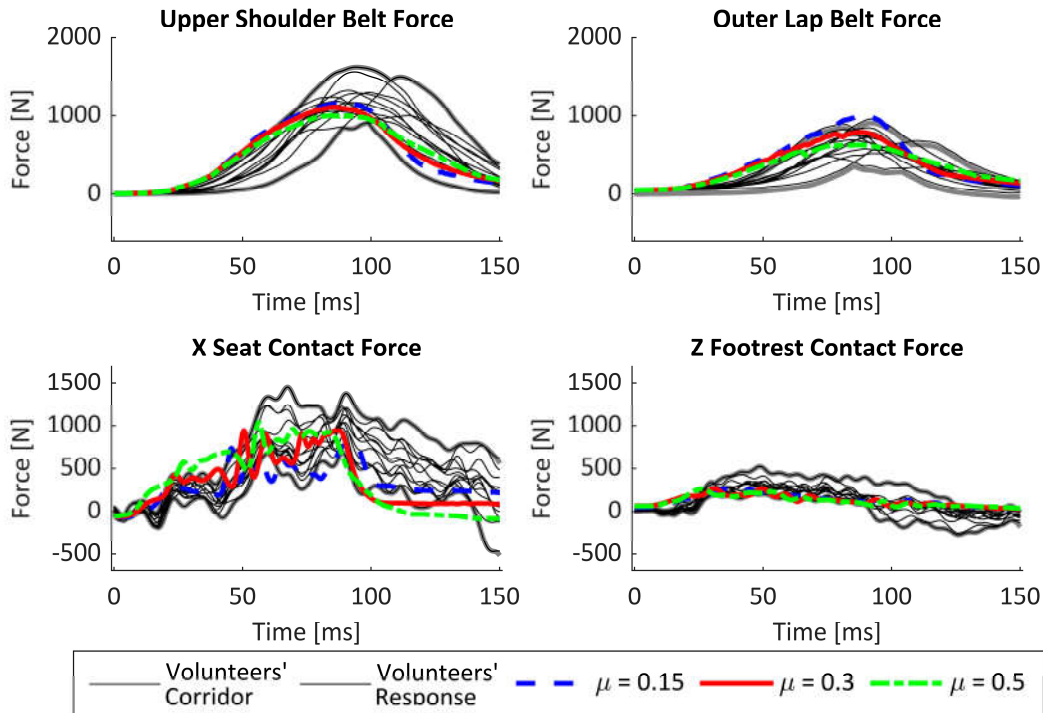
Figure 5. Plot of shoulder and lap belt forces and contact forces of the seat and footrest.
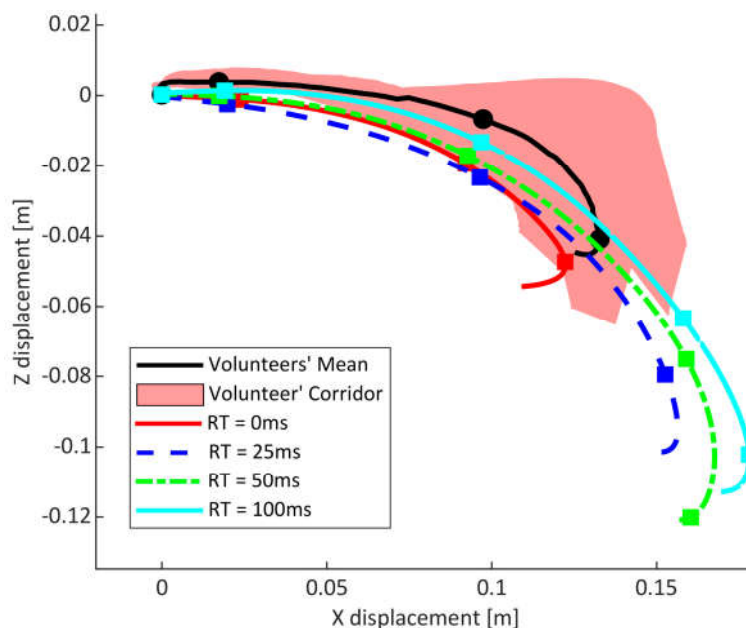
Figure 6. Head centre of gravity displacement of volunteers and active HBM with RT equal to 0, 25, 50, and 100ms. The circle (volunteers) and square (simulations) markers detail the head displacement every 50ms.

Testing of HBM neck co-contraction

In addition to the simulation with RT=0ms and no CCR, five simulations were performed with different combinations of RT and CCR. The simulations with no CCR and RT=0ms and with either half or full CCR and RT=25ms showed the best correlation with the volunteers' forward peak forward excursion and timing of the peak with [133mm; 153ms], [145mm; 158ms], and [149mm; 161ms], respectively. In the downward excursion, an increment in the CCR level reduced the peak value observed with the largest reductions in the cases of RT equal to 25ms, which predicted [75mm; 177ms] and [61mm; 170ms] with half and full CCR levels, respectively. Figure 7 shows the head displacements predicted by the different combinations of CCR and RT.
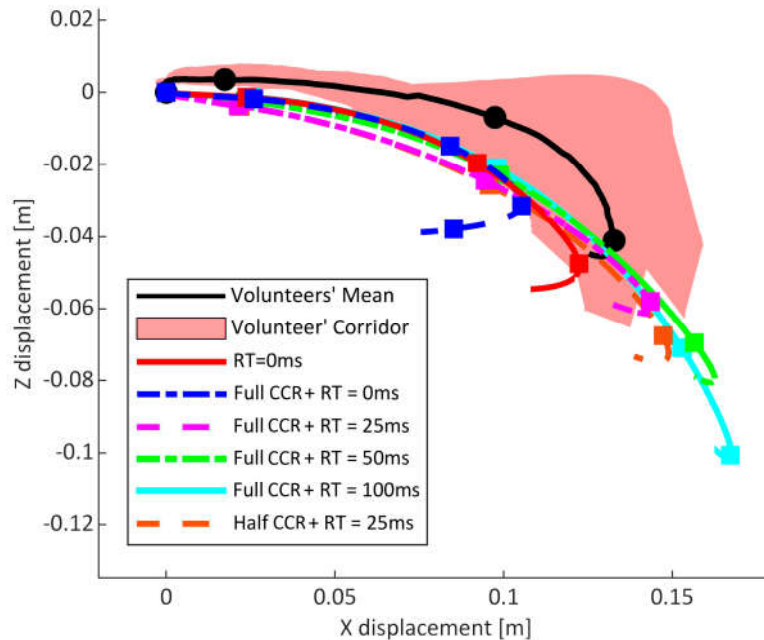

Figure 7. Head centre of gravity displacement of volunteers and active HBM for different combinations of CCR and RT. The circle (volunteers) and square (simulations) markers detail the head displacement every 50ms.
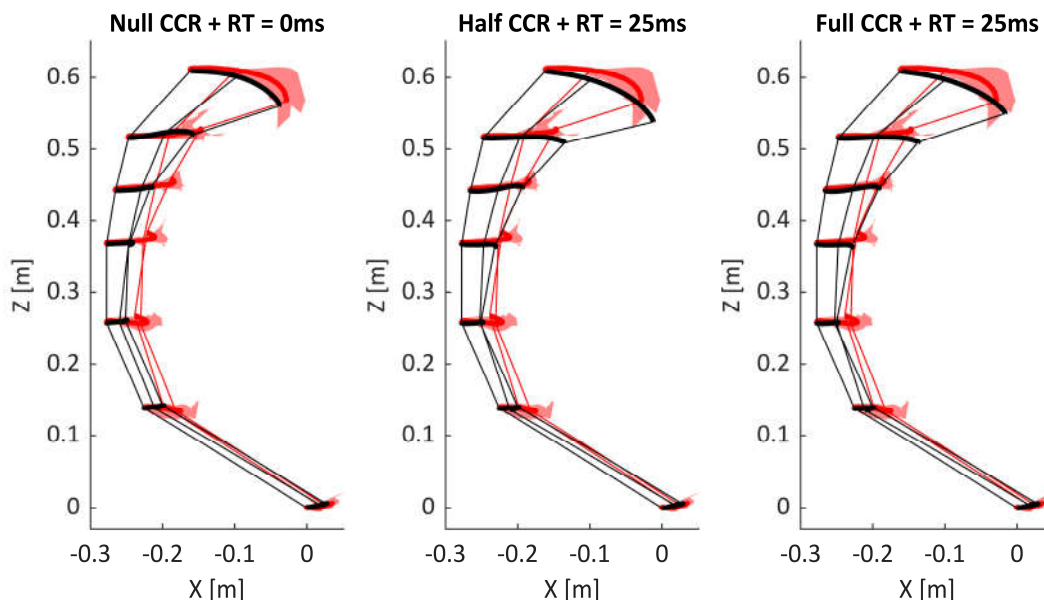

Figure 8. Trajectories of reflective markers (head, C4, T1, T4, T8, and T12 vertebra, and hip) for the volunteers' mean (red line), and simulations (black line) with: RT=0ms and null CCR; and RT=25ms with half and full CCR. Thin lines linked the marker positions each 80ms and red shaded areas describe the volunteers' corridor.

Figure 8 shows the trajectories of the reflective markers for the head, C4, T1, T4, T8, and T12 vertebra, and hip joint for the volunteers' mean and the simulations with no CCR and RT=0ms and half and full CCR with RT=25ms. As is shown, the HBM head and C4 vertebrae trajectories matched the bottom side of the volunteers' corridor. However, the forward excursion of the vertebra T4, T8 and T12 was underpredicted by the HBM. The mean volunteers' forward excursions were 68±13mm, 58±13mm, and 53±13mm, respectively, which were

underpredicted by 25-50% (17-30mm) at the T4 vertebrae and by 50% (23-28mm) at the T8 and T12 vertebra.

Figure 9 shows the volunteers' corridors for the head angular acceleration and the neck response (Fx, Fz, and My) measured at the occipital-condyle junction, which were obtained through the CORA method, and the results of the following configurations: null CCR with RT=0ms; full CCR with RT=0ms; full CCR with RT=25ms; and half CCR with RT=25ms. Although the peak angular head accelerations obtained with the active HBMs were lower than that measured in the volunteers, the neck moment showed a fair to good correlation (CORA = [0.688, 0.45, 0.755, 0.602], respectively). Similar results were obtained for the neck tangential force with fair correlations (CORA = [0.702, 0.655, 0.556, 0.48], respectively). The four cases showed a good prediction of the mean peak value (difference <5%), however a RT=25ms resulted in an overprediction of the timing of the peak (increasing between 15-20ms) and duration of the peak. The largest difference between the active HBM and the volunteers' response was in the neck axial force. In this case the HBM predicted a tensile force before the maximum forward excursion was reached, while the volunteer's mean behaviour was in compression in the same period of time.
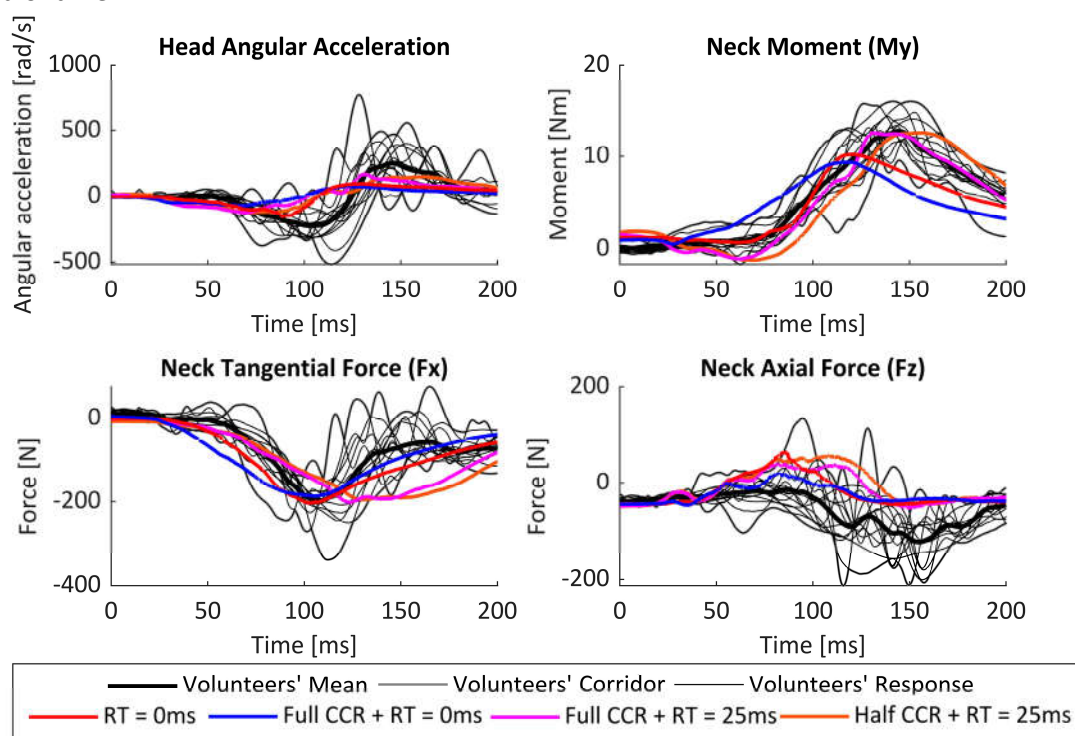

Figure 9. Head angular acceleration and neck response of volunteers and simulations with: no CCR + RT=0ms; full CCR + RT=0ms; full CCR + RT=25ms; and half CCR + RT=25ms.

IV. Discussion

Eleven simulations were carried out in three groups to assess the kinematic and dynamic response of the Madymo active HBM with a new set of kinematic data corresponding to frontal deceleration tests at 9km/h. The first group of simulations had the objective of calibrating the model and assessing the influence of the friction coefficient between the seat and the HBM. These simulations showed that the friction coefficient had a small influence over the excursion of several landmarks of the model. Regardless of the value of the friction coefficient, the HBM hip-joint showed smaller displacements than the corresponding landmark in the volunteers. A similar result had been reported in [13], using a similar setup and acceleration pulse. The difference was attributed to the potential sliding motion of the pelvis over the flesh, a phenomenon that is not modelled in the HBM. Lap belt loads showed the largest sensitivity to the value changes of the friction coefficient, but the peak values were within or close to the volunteers' corridor. Therefore, a friction coefficient equal to 0.3 was chosen to carry out the rest of the simulations.

Different RTs with null CCR were simulated in the second group of simulations, which resulted always in an overprediction of the volunteers' head excursion for RT higher than 0ms. This difference could be attributed to two factors: the model, where a leverage of the PID parameters could enhance the prediction maintaining a null or low CCR levels and RT higher than 0ms; and the volunteers, where the difference could be the result of some

CCR level in the volunteers since they were aware of the impact. Thus, the third group of simulations contained different combinations of RT and CCR to investigate further this hypothesis. In this case, the analysis of the spine reflective markers and the dynamics of the neck response were also included. Higher levels of CCR of the neck muscles showed a reduction of the head excursion, which was greater with low RTs (e.g., the vertical excursion reduction with RT=100ms was 20% and lower than 1% for the horizontal, but with RT=25ms the reduction was 40% and 10%, respectively, with full CCR). However, a full level of CCR of the neck muscles, which was used to obtain the reduction in the head excursion with 50ms and 100ms, also did not match the relaxed condition in which the volunteers were instructed.

Figure 10 and 11 in the appendix show the volunteers' mean response and corridor and the predictions obtained for the second and third group of simulations with the CORA method. As Figure 11 shows, the model predicted head horizontal displacements with a deviation of 20% or less from the volunteers' corridor for all cases, similar to the obtained in [13], with fair to good ratings obtained in the correlation analysis (i.e., 8.6≥CORA≥4.4). However, the vertical displacements showed larger variability in the volunteers' response than in the horizontal direction. While the volunteers' mean peak downward excursion was 47±17mm, the minimum and maximum downward excursions were 22 and 89mm, with three volunteers experimenting a larger excursion than 64mm. Therefore, although the HBM configuration with RT=0ms and null CCR was the one that provided the best approximation to the volunteers' average response, the configuration with RT=25ms and half CCR levels predicted an excursion similar to the volunteers with larger displacements. Futures studies should focus on the effect that a larger downward displacement has on injury risk.

The analysis of the vertical head displacement within the first 100ms showed an upward head movement, which was not predicted in any simulation, as shown in Figure 7 and Figure 11. It was hypothesized that this behaviour was the result of an underprediction in the forward excursion of the spine markers (T4, T8, and T12 vertebrae markers) reducing spine straightening, and therefore reducing the upward displacement of the T1 and C4 vertebra and the head. This effect was observed in the trajectory of these markers and in the prediction of the neck axial force, which showed a tensile force in all HBM configurations near the maximum forward head excursion while the volunteers showed a compression force at the occipital-condyle junction during the whole experiment. Moreover, the spine curvature at the beginning of the acceleration pulse could also influence this response. However, the priority in the positioning procedure was to match the same initial hip and head position observed in the volunteers with less consideration on the initial position of the vertebra.

The findings in this study are subjected to at least two limitations. First, the anthropometric differences between the volunteers and the HBM, which could explain the differences in the initial positions of the vertebrae markers. And second, the simplifications applied to the model, which were: *i*) the constraints in the parameters of the model that could not be modified due to their encryption, as the PID controller of the neck muscles; *ii*) the levels of muscle activation were considered constant with full activation, because lower activation levels could results in larger excursion than the obtained in this study; *iv*) the values of RT and CCR were considered constant through the whole simulation; and *v*) the RT values were considered the same for all muscle controllers.

The validation of active HBMs usually relies on forward excursions measured in volunteers' experiments, which could affect injury risk after a pre-crash event as was studied in Saito et al. [7]. However, the downward head excursion could be also important to predict the interaction with safety devices, and therefore the injury risk. In the literature some studies reported vertical head displacements, but the predictions for these were always less accurate than those predicted for horizontal displacement [6,16,31,32]. Furthermore, it was found in this study that the downward head excursion is more sensitive to variations in the muscle behaviour than the forward excursion. Therefore, the calibration of the neck muscle controller could rely more in the vertical displacement than in the horizontal ensuring that the final position is closer to the volunteers' response.

V. CONCLUSIONS

This study focused on extend the current validation of the Madymo active HBM. It was found that while variations in the response time delay and the co-contraction of the neck muscles could cause similar forward excursions, this could also derive in an overprediction of the downward excursions; and therefore, their election should not rely only in the forward excursion. Furthermore, differences in spine excursion were predicted in the HBM which affected the vertical head displacements and neck force and moment response. Therefore, future

studies should focus on the MADYMO active HBM spine to understand the causes of lower forward excursion; the optimization process applied to the neck controller taking into account RT, CCR levels, and the PID controller to enhance the model prediction in low-acceleration impacts; and the effect of different downward head excursions on the injury risk.

VI. ACKNOWLEDGEMENT

VII. REFERENCES

[1]   Hu, J., Flannagan, C.A., Bao, S., McCoy, R.W., Siasoco, K.M., and Barbat, S. (2015) Integration of active and passive safety technologies-a method to study and estimate field capability. Stapp Car Crash Journal, 59 269–296.

[2]   Iraeus, J. and Lindquist, M. (2016) Development and validation of a generic finite element vehicle buck model for the analysis of driver rib fractures in real life nearside oblique frontal crashes. *Accident Analysis & Prevention*, 95 42–56.

[3]   Hu, J., Zhang, K., Reed, M.P., Wang, J.-T., Neal, M., and Lin, C.-H. (2019) Frontal crash simulations using parametric human models representing a diverse population. *Traffic Injury Prevention*, 20 (sup1), S97–S105.

[4]   Perez-Rapela, D., Forman, J.L., Huddleston, S.H., and Crandall, J.R. (2020) Methodology for vehicle safety development and assessment accounting for occupant response variability to human and non-human factors. *Computer Methods in Biomechanics and Biomedical Engineering*, 1–16.

[5]   Joodaki, H., Gepner, B., and Kerrigan, J. (2020) Leveraging machine learning for predicting human body model response in restraint design simulations. *Computer Methods in Biomechanics and Biomedical Engineering*, 1–15.

[6]   Östh, J., Brolin, K., and Bråse, D. (2015) A human body model with active muscles for simulation of pretensioned restraints in autonomous braking interventions. *Traffic Injury Prevention*, 16 (3), 304–313.

[7]   Saito, H., Matsushita, T., Pipkorn, B., and Boström, O. (2016) Evaluation of frontal impact restraint system in integrated safety scenario using human body model with PID controlled active muscles. *Proceedings of the International Conference on Biomechanics of Impact IRCOBI*, Malaga, Spain.

[8]   Arbogast, K.B., Balasubramanian, S., et al. (2009) Comparison of kinematic responses of the head and spine for children and adults in low-speed frontal sled tests. *Stap Car Crash Journal*, 53 329–72.

[9]   Balasubramanian, S., Seacrist, T., et al. (2009) Head and spinal trajectories in children and adults exposed to low speed frontal acceleration. *International Technical Conference on the Enhanced Safety of Vehicles*.

[10]   Seacrist, T., Arbogast, K.B., et al. (2011) Kinetics of the cervical spine in pediatric and adult volunteers during low speed frontal impacts. *Journal of Biomechanics*, 45 (1), 99–106.

[11]   Beeman, S.M., Kemper, A.R., Madigan, M.L., Franck, C.T., and Loftus, S.C. (2012) Occupant kinematics in low-speed frontal sled tests: Human volunteers, Hybrid III ATD, and PMHS. *Accident Analysis & Prevention*, 47 128–139.

[12]   Sato, F., Nakajima, T., Ono, K., Svensson, M., Brolin, K., and Kaneoka, K. (2014) Dynamic cervical vertebral motion of female and male volunteers and analysis of its interaction with head/neck/torso behavior during low-speed rear impact. *Proceedings of the International Conference on Biomechanics of Impact IRCOBI*, pp. 10–12.

[13]   Meijer, R., Elrofai, H., Broos, W., and Hassel, E. van (2013) Evaluation of an active multi-body human model for braking and frontal crash events. *23rd International Technical Conference on the Enhanced Safety of Vehicles (ESV) National Highway Traffic Safety Administration*, Seoul, Korea.

[14]   Iwamoto, M., Nakahira, Y., and Kimpara, H. (2015) Development and validation of the total human model for safety (THUMS) toward further understanding of occupant injury mechanisms in precrash and during crash. *Traffic Injury Prevention*, 16 (sup1), S36–S48.

[15]   Kato, D., Nakahira, Y., Atsumi, N., and Iwamoto, M. (2018) Development of human-body model THUMS Version 6 containing muscle controllers and application to injury analysis in frontal collision after brake

deceleration. *Proceedings of the International Research Council on Biomechanics of Injury (IRCOBI)*, Athens, Greecepp. 12–14.

[16] Putra, I.P.A., Iraeus, J., Thomson, R., Svensson, M.Y., Linder, A., and Sato, F. (2019) Comparison of control strategies for the cervical muscles of an average female head-neck finite element model. *Traffic Injury Prevention*, 20 (sup2), S116–S122.

[17] Devane, K., Johnson, D., and Gayzik, F.S. (2019) Validation of a simplified human body model in relaxed and braced conditions in low-speed frontal sled tests. *Traffic Injury Prevention*, 20 (8), 832–837.

[18] Kato, D., Nakahira, Y., and Iwamoto, M. (2017) A study of muscle control with two feedback controls for posture and reaction force for more accurate prediction of occupant kinematics in low-speed frontal impacts. *Proceedings of the 25th ESV Conference*, pp. 5–8.

[19] Nemirovsky, N., Van Rooij, L., and others (2010) A new methodology for biofidelic head-neck postural control. *Proceedings of the International Conference on Biomechanics of Impact IRCOBI*, Hanover, Germany.

[20] Meijer, R., Van Hassel, E., Broos, J., Elrofai, H., Van Rooij, L., and Van Hooijdonk, P. (2012) Development of a multi-body human model that predicts active and passive human behaviour. *Proceedings of the International Conference on Biomechanics of Impact IRCOBI*, Dublin, Irelandpp. 622–636.

[21] Meijer, M., Broos, J., Elrofai, H., de Bruijn, E., Forbes, P., and Happee, R. (2013) Modelling of bracing in a multi-body active human model. *Proceedings of the International Conference on Biomechanics of Impact IRCOBI*, Gothenburg, Sweden.

[22] Vives-Torres, C.M., Valdano, M., et al. (2021) Comparison of upper neck loading in young adult and elderly volunteers during low speed frontal impacts. *Frontiers in Bioengineering and Biotechnology (In Revision Process)*.

[23] Muehlbauer, J., Schick, S., Draper, D., Lopez-Valdes, F.J., Symeonidis, I., and Peldschus, S. (2019) Feasibility study of a safe sled environment for reclined frontal deceleration tests with human volunteers. *Traffic Injury Prevention*, 20 (sup2), S171–S174.

[24] Lopez-Valdes, F.J., Mroz, K., et al. (2018) Chest injuries of elderly postmortem human surrogates (PMHSs) under seat belt and airbag loading in frontal sled impacts: Comparison to matching THOR tests. *Traffic Injury Prevention*, 19 (sup2), S55–S63.

[25] Eggers, A., Ott, J., et al. (2017) A new generic frontal occupant sled test set-up developed within the EU-project SENIORS. *Proceedings of Conference on the Enhancement of Safety Vehicles (ESV)*, Detroit, USA.

[26] Lopez-Valdes, F.J., Lau, A., et al. (2010) Analysis of spinal motion and loads during frontal impacts. Comparison between PMHS and ATD. *Annals of Advances in Automotive Medicine/Annual Scientific Conference*, p. 61.

[27] SAE (2007) Instrumentation for impact test: Part 1 - electronic instrumentation compiled by SAE international.

[28] "Frontal Sled – SENIORS – TUC-Project", https://tuc-project.org/frontal-sled-seniors/.

[29] Gehre, C. and Stahlschmidt, S. (2011) Assessment of dummy models by using objective rating methods. *22nd International Technical Conference on the Enhanced Safety of Vehicles Conference (ESV)*, Washington, D.C., USA.

[30] Gehre, C., Gades, H., and Wernicke, P. (2009) Objective rating of signals using test and simulation responses. Proceedings: International Technical Conference on the Enhanced Safety of Vehicles, National Highway Traffic Safety Administration, Stuttgart, Germany.

[31] Östh, J., Mendoza-Vazquez, M., Linder, A., Svensson, M.Y., and Brolin, K. (2017) The VIVA OpenHBM finite element 50th percentile female occupant model: whole body model development and kinematic validation. *Proceedings of the International Conference on Biomechanics of Injury IRCOBI*, Antwerp, Belgiumpp. 13–15.

[32] Östh, J., Brolin, K., Carlsson, S., Wismans, J., and Davidsson, J. (2012) The occupant response to autonomous braking: a modeling approach that accounts for active musculature. *Traffic Injury Prevention*, 13 (3), 265–277.
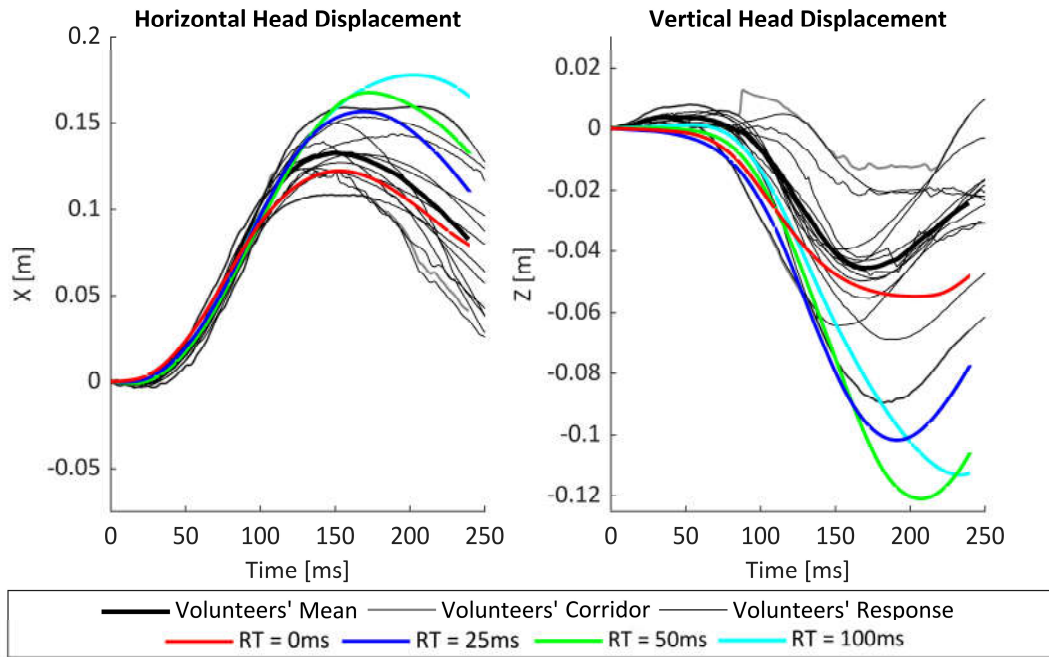
VIII. APPENDIX

Figure 10. Head kinematics of the MADYMO active HBM with null CCR of the neck muscles in a frontal impact simulation compared with that 13 volunteers [22].
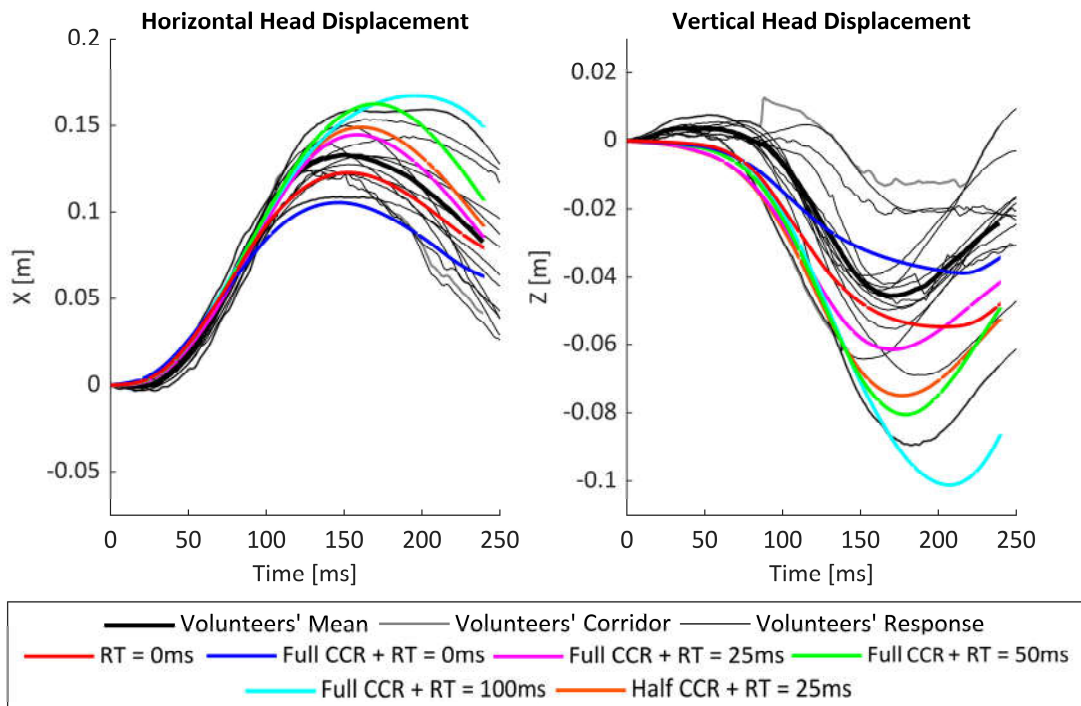

Figure 11. Head kinematics of the MADYMO active HBM with different combination of levels of CCR of the neck muscles and RTs in a frontal impact simulation compared with that 13 volunteers [22].

TABLE IV
OBJECTIVE RATING RESULTS AND CONFIGURATION OF MADYMO ACTIVE HBM SIMULATIONS

Simulation	Friction coefficient	RT (ms)	CCR	Total	Head X	Head Z	C4 X	C4 Z	T1 X	T1 Z	T4 X	T4 Z	T8 X	T8 Z	T12 X	T12 Z	Hip X	Hip Z	Rot Y acc	Fx	Fz	My	Upper Shoulder Belt	Lower Shoulder Belt	Inner Lap Belt	Outer Lap Belt	X Seat Contact Force	Z Left Footrest Contact Force	Z Right Footrest Contact Force
1	0.3	0	No	0.478	0.718	0.626	0.584	0.308	0.469	0.259	0.467	0.081	0.47	0.307	0.6	0.397	0.814	0.684	0.592	0.702	0.368	0.688	0.678	0.607	0.531	0.591	0.483	0.437	0.482
2	0.15	0	No	0.471	0.666	0.601	0.549	0.307	0.462	0.279	0.455	0.049	0.446	0.292	0.537	0.409	0.799	0.662	0.598	0.691	0.377	0.684	0.675	0.655	0.478	0.609	0.591	0.514	0.548
3	0.5	0	No	0.488	0.77	0.672	0.676	0.3	0.486	0.297	0.481	0.158	0.487	0.31	0.634	0.298	0.7	0.71	0.592	0.709	0.348	0.706	0.682	0.601	0.539	0.599	0.421	0.425	0.416
4	0.3	25	No	0.435	0.695	0.4	0.806	0.258	0.645	0.259	0.586	0.024	0.561	0.261	0.633	0.387	0.766	0.669	0.712	0.496	0.308	0.418	0.577	0.545	0.507	0.534	0.544	0.445	0.403
5	0.3	50	No	0.479	0.712	0.413	0.691	0.222	0.746	0.391	0.656	0.134	0.624	0.392	0.645	0.41	0.735	0.688	0.524	0.519	0.314	0.365	0.589	0.561	0.521	0.563	0.481	0.45	0.402
6	0.3	100	No	0.517	0.706	0.535	0.627	0.224	0.59	0.541	0.624	0.283	0.607	0.412	0.576	0.313	0.674	0.725	0.547	0.767	0.267	0.483	0.688	0.622	0.568	0.649	0.446	0.524	0.522
7	0.3	0	Full	0.459	0.466	0.643	0.468	0.349	0.45	0.317	0.454	0.095	0.467	0.314	0.586	0.368	0.792	0.686	0.363	0.655	0.469	0.45	0.671	0.608	0.528	0.603	0.47	0.455	0.484
8	0.3	25	Full	0.445	0.815	0.468	0.84	0.174	0.729	0.266	0.647	0.027	0.595	0.257	0.612	0.417	0.743	0.686	0.433	0.556	0.326	0.755	0.57	0.525	0.514	0.534	0.541	0.435	0.382
9	0.3	50	Full	0.479	0.593	0.413	0.627	0.37	0.63	0.419	0.64	0.141	0.617	0.388	0.626	0.377	0.716	0.697	0.42	0.475	0.31	0.466	0.582	0.548	0.528	0.571	0.501	0.456	0.419
10	0.3	100	Full	0.485	0.584	0.422	0.561	0.232	0.565	0.477	0.606	0.306	0.609	0.409	0.599	0.321	0.655	0.721	0.393	0.559	0.244	0.418	0.632	0.593	0.572	0.645	0.424	0.563	0.528
11	0.3	25	Half	0.436	0.729	0.388	0.811	0.21	0.719	0.247	0.629	0.031	0.577	0.258	0.617	0.398	0.754	0.68	0.502	0.48	0.285	0.602	0.568	0.528	0.522	0.536	0.54	0.437	0.387